Cyclotrimerization Reactions Catalyzed by Rhodium(I) Half-Sandwich Complexes: A Mechanistic Density Functional Study

Laura Orian,*,† Joost N. P. van Stralen,‡ and F. Matthias Bickelhaupt*,‡

Dipartimento di Scienze Chimiche, Università degli Studi di Padova, Via Marzolo 1, 35129 Padova, Italy, and Afdeling Theoretische Chemie, Scheikundig Laboratorium der Vrije Universiteit, De Boelelaan 1083, NL-1081 HV Amsterdam, The Netherlands

Received May 10, 2007

We propose and examine a comprehensive mechanism of the [(η^5-C_5H_5)Rh]-catalyzed [2+2+2] cycloadditions of acetylene to benzene and of acetylene and acetonitrile to 2-methylpyridine, based on an extensive and detailed exploration of the potential energy surfaces using density functional theory. Both processes involve the formation of a coordinatively unsaturated 16-electron metallacycle, occurring after the replacement of the ancillary ligands L of the catalyst precursor of general formula [(η^5-C_5H_5)-RhL_2] (typically L = C_2H_4, CO, PH_3 or L_2 = 1,5-cyclooctadiene) by two acetylene molecules. The facile coordination of a third acetylene molecule, and its subsequent addition to the π electron system of the rhodacycle, leads to the formation of an intermediate, which is characterized by a six-membered arene ring coordinated to the metal in η^4 fashion. The release of benzene occurs by stepwise addition of two acetylene molecules, which regenerates the catalyst. In the presence of acetonitrile, a nitrile molecule coordinates to the rhodacycle, and different stages are outlined for the process, leading to the eventual release of 2-methylpyridine. The steric and electronic effects of the π ligand coordinated to the metal are also included in our exploration by addressing the whole mechanism of the [(η^5-C_9H_7)Rh]-catalyzed alkyne self-trimerization to benzene. The kinetic parameters, i.e., the energies in vacuum and in different solvents, and the geometries of the intermediates and of the transition states are analyzed in detail.

1. Introduction

Cyclizations of unsaturated molecules are intensively studied reactions since they potentially afford a variety of substituted benzenes, heterocyclic and polycyclic compounds of paramount importance in chemical industry and pharmaceutical research.[1] The simplest examples are the one-step formation of the C−C bonds of benzene by acetylene trimerization and the cycloaddition of nitriles with 2 equiv of acetylene, which is a versatile and effective method for the synthesis of 2-alkylpyridines (Scheme 1).

Scheme 1

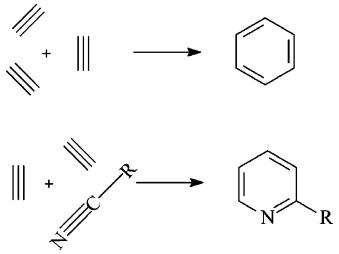

The cyclotrimerization process can be conveniently carried out in the presence of a metal-based catalyst under mild conditions, in contrast to the purely thermal variant, which is disfavored by a rather high activation energy and especially by the decrease in entropy associated with bringing three reactants together.[2]

While the fundamental research of Wakatsuki and Yamazaki,[3] Bönnemann,[4] and Vollhardt[5] established that cobalt-based catalysts are the compounds of primary choice for the [2+2+2] cyclizations, numerous studies have demonstrated that several different transition metal complexes possess discrete catalytic efficiencies.[6]

Unfortunately, chemoselectivity and regioselectivity issues limit the synthetic usefulness of this class of reactions. For instance, most catalysts capable of promoting the synthesis of pyridine are also capable of promoting alkyne homotrimerization, which leads to the formation of benzene derivatives. Detailed theoretical knowledge of the reaction mechanism together with empirical information from experimental studies might help to accurately design novel catalysts able to control the combination of the reactants in order to improve the chemoselectivity and the yields.

Albright[7] and co-workers first provided a rigorous and detailed computational description of the whole mechanism of

* Corresponding authors. Fax: +39 0498275239. E-mail: laura.orian@unipd.it. Fax: +31 20 59 87 629. E-mail: fm.bickelhaupt@few.vu.nl.

† Università degli Studi di Padova.

‡ Vrije Universiteit.

(1) (a) Jones, G. Pyridines and Their Benzoderivatives: Synthesis. In *Comprehensive Heterocyclic Chemistry II*; Katritzky, A., Rees, C. W., Scriven, E. F. V., Eds.; Pergamon: Oxford, 1996; Vol. 5, pp 167−243. (b) Curran, D. P. *Advances in Cycloaddition*; JAI Press: Greenwich, CT, 1994; Vols. 1−3. (c) Trost, B. M. *Angew. Chem., Int. Ed. Engl.* **1985**, *34*, 259.

(2) (a) The conversion of three acetylene molecules into benzene is kinetically prohibited: Dower, W. V.; Vollhardt, K. P. C. *J. Am. Chem. Soc.* **1982**, *104*, 6878. (b) The enthalpy of activation is responsible for the reluctance of acetylene to self-trimerize thermally: Houk, K. N.; Gandour, R. W.; Strozier, R. W.; Randon, N. G.; Paquette, L. A. *J. Am. Chem. Soc.* **1979**, *101*, 6797. (c) Back, H. M. *Can. J. Chem.* **1971**, *49*, 2199.

(3) (a) Wakatsuki, Y.; Yamazaki, H. *J. Chem. Soc., Chem. Commun.* **1973**, 280. (b) Wakatsuki, Y.; Yamazaki, H. *Bull. Chem. Soc. Jpn.* **1985**, *58*, 2715.

(4) (a) Bönnemann, H. *Angew. Chem., Int. Ed. Engl.* **1978**, *17*, 505. (b) Bönnemann, H. *Angew. Chem., Int. Ed. Engl.* **1985**, *24*, 248.

(5) (a) Vollhardt, K. P. C. *Acc. Chem. Res.* **1977**, *10*, 1. (b) Vollhardt, K. P. C. *Angew. Chem., Int. Ed. Engl.* **1984**, *23*, 539.

(6) (a) Lautens, M.; Klute, W.; Tam, W. *Chem. Rev.* **1996**, *96*, 49. (b) Varela, J. A.; Saá, C. *Chem. Rev.* **2003**, *103*, 3787. (c) Chopade, P. R.; Louie, J. *Adv. Synth. Catal.* **2006**, *348*, 2307. (d) Kotha, S.; Brahmachar, E.; Lahni, K. *Eur. J. Org. Chem.* **2005**, 4741.

10.1021/om7004222 CCC: $37.00
Publication on Web 06/19/2007

acetylene trimerization catalyzed by the CpCo ($Cp = C_5H_5$) fragment. Gandon and Vollhardt[8] extended the approach to the cobalt-mediated synthesis of cyclohexadiene from acetylene and ethylene. More recently Koga[9] et al. explored theoretically the regioselectivity of the first step of the CpCo-catalyzed acetylene trimerization and reexamined the work by Albright,[7] addressing different mechanistic schemes in both the singlet and triplet state. Accurate computational studies for the same reactions and the cocyclization of acetylene and CS_2 have been carried out by Kirchner[10] and co-workers with CpRuCl as catalyst.

Very recently Dazinger et al.[11] proposed a DFT mechanism of the CpRuCl-catalyzed synthesis of pyridine from acetylene and HCN, reexamining the previous work by Yamamoto and co-workers.[12] In their discussion, part of the mechanism of the same reaction catalyzed by CpCo and CpRh fragments is included.

Due to the great interest in the chemical reactivity of rhodium complexes, especially in terms of their suitability for catalytic systems, we present in this paper the results of a theoretical investigation on the mechanism of [(η^5-C_5H_5)Rh]-catalyzed cyclotrimerization of acetylene to benzene and cocyclotrimerization of acetylene and acetonitrile to 2-methylpyridine. All calculations have been carried out using density functional theory (DFT) at the BLYP/TZ2P level as implemented in the ADF program.[13−15] We compare the gas-phase model reactions with the corresponding mechanisms in acetonitrile as well as toluene solution using the COSMO approach for treating solvent effects.[16]

The catalytic efficiency of half-sandwich Rh(I) fragments toward cyclization reactions has been experimentally assessed by Ingrosso[17] and co-workers. They have found that complexes of general formula $CpRhL_2$ ($L = CO$, C_2H_4; $L_2 = COD$, i.e., 1,5-cyclooctadiene) are long-lived efficient catalyst precursors for the synthesis of pyridine derivatives by cocyclization of several different alkynes and nitriles. They were able to control successfully the concurrent formation of benzene from alkyne self-trimerization. High pyridine yields (above 80%) can be obtained at a temperature between 100 and 150 °C, in the absence of solvent and driving the chemoselectivity in favor of pyridine by increasing the nitrile-to-alkyne molar ratio to 5:1 or 8:1. Adopting these optimum reaction conditions, benzene yields were found to drop significantly.

The mechanism of CpRh-catalyzed homotrimerization of acetylene is intrinsically important for the synthesis of polysubstituted benzenes.[18] The outlined stages and the energetics of this process are here compared to the theoretical results obtained for cobalt- and ruthenium-catalyzed acetylene cyclotrimerizations, in order to gain insight into the interplay between the size (covalent atomic radius) and the valence electron configuration of the metal core mediating these mechanisms. In addition, since the cocyclization of acetylene and acetonitrile is always accompanied by the formation of differing amounts of arene arising from alkyne self-trimerization, the competition between the two processes is discussed.

Finally, the catalytic activity of the [(η^5-C_9H_7)Rh] fragment is explored. Despite the great importance of indenyl (Ind = C_9H_7) complexes, which are well known for their reactivity ("indenyl effect"),[19] this study is, to the best of our knowledge, the first one that addresses the mechanism of cyclotrimerization reactions catalyzed by indenyl−metal complexes.

2. Methods

2.1. Computational Details. All density functional theory (DFT)[13] calculations have been done with the Amsterdam Density Functional (ADF) program.[14,15] Calculations were done with scalar relativistic effects accounted for using the zeroth-order regular approximation (ZORA).[20] The BLYP[21] density functional was used, in combination with the TZ2P basis set for all elements. The TZ2P basis set is a large uncontracted set of Slater-type orbitals (STOs), is of triple-ζ quality, and has been augmented with two sets of polarization functions on each atom: 2p and 3d in the case of H, 3d and 4f in the case of C and N, and 5p and 4f in the case of Rh. An auxiliary set of s, p, d, f, and g STOs was used to fit the molecular density and to represent the Coulomb and exchange potentials accurately in each SCF cycle.[14] The frozen-core approximation was employed: up to 1s for C and N and up to 3d for Rh. The electronic structures of the intermediates and transition-state geometries were analyzed in terms of the quantitative molecular orbital (MO) model contained in Kohn−Sham DFT.[22] Recently, it has been shown that our approach is in satisfactory agreement with high-level *ab initio* calculations for oxidative addition reactions of the C−H,[23] C−C,[24] C−F,[25] and C−Cl[26] bonds to palladium.

Equilibrium and transition-state geometries were fully optimized (i.e., without any symmetry restriction) using analytical gradient techniques. All structures were verified by frequency calculations: for minima all normal modes have real frequencies, whereas transition states have one normal mode with an imaginary frequency. The character of the normal mode associated with the

(7) Hardesty, J. H.; Koerner, J. B.; Albright, T. A.; Lee, G.-Y. *J. Am. Chem. Soc.* **1999**, *121*, 6055.
(8) Gandon, V.; Agenet, N.; Vollhardt, P. C.; Malacria, M.; Aubert, C. *J. Am. Chem. Soc.* **2006**, *128*, 8509.
(9) (a) Dehy, A. A; Koga, N. *Bull. Chem. Soc.* **2005**, *78*, 781. (b) Dehy, A. A.; Suresh, C. H.; Koga, N. *Bull. Chem. Soc.* **2005**, *78*, 792.
(10) Kirchner, K.; Calhorda, M. J.; Schmid, R.; Veiros, L. F. *J. Am. Chem. Soc.* **2003**, *125*, 11721.
(11) Dazinger, G.; Torres-Rodrigues, M.; Kirchner, K.; Calhorda, M. J.; Costa, P. J. *J. Organomet. Chem.* **2006**, *691*, 4434.
(12) Yamamoto, K.; Kinpara, K.; Saigoku, T.; Takagishi, H.; Okuda, S.; Nishiyama, H.; Itoh, K. *J. Am. Chem. Soc.* **2005**, *127*, 605.
(13) (a) Hohenberg, P.; Kohn, W. *Phys. Rev.* **1964**, *136*, B864. (b) Kohn, W.; Sham, L. J. *Phys. Rev.* **1965**, *140*, A1133. (c) Parr, R. G.; Yang, W. *Density-Functional Theory of Atoms and Molecules*; Oxford University Press: New York, 1989.
(14) Baerends, E. J.; Ellis, D. E.; Ros, P. *Chem. Phys.* **1973**, *2*, 41.
(15) (a) te Velde, G.; Bickelhaupt, F. M.; Baerends, E. J.; Fonseca Guerra, C.; van Gisbergen, S. J. A.; Snijders, J. G.; Ziegler, T. *J. Comput. Chem.* **2001**, *22*, 931. (b) Baerends, E. J.; et al. Computer code *ADF2006.01*; SCM, Theoretical Chemistry, Vrije Universiteit: Amsterdam, The Netherlands, 2006.
(16) (a) Klamt, A.; Schüürmann, G. *J. Chem. Soc., Perkin Trans. 2* **1993**, 799. (b) Klamt, A. *J. Phys. Chem.* **1995**, *99*, 2224.
(17) (a) Cioni, P.; Diversi, P.; Ingrosso, G.; Lucherini, A.; Ronca, P. *J. Mol. Catal.* **1987**, *40*, 337. (b) Diversi, P.; Ermini, L.; Ingrosso, G.; Lucherini, A. *J. Organomet. Chem.* **1993**, *447*, 291.
(18) Saito, S.; Yamamoto, Y. *Chem. Rev.* **2000**, *100*, 2901.
(19) Rerek, M. E.; Ji, L.-N.; Basolo, F. *J. Chem. Soc., Chem. Commun.* **1983**, 1208.
(20) van Lenthe, E.; Baerends, E. J.; Snijders, J. G. *J. Chem. Phys.* **1994**, *101*, 9783.
(21) (a) Becke, A. D. *Phys. Rev. A* **1988**, *38*, 3098. (b) Lee, C.; Yang, W.; Parr, R. G. *Phys. Rev. B* **1988**, *37*, 785.
(22) (a) Bickelhaupt, F. M.; Baerends, E. J. Kohn-Sham density functional theory: Predicting and understanding chemistry. In *Reviews in Computational Chemistry*; Lipkowitz, K. B., Boyd, D. B., Eds.; VCH Publishers Inc.: New York, 2000; Vol. 15; p 1. (b) Bickelhaupt, F. M.; Nibbering, N. M. M.; van Wezenbeek, E. M.; Baerends, E. J. *J. Phys. Chem.* **1992**, *96*, 4864. (c) Ziegler, T.; Rauk, A. *Theor. Chim. Acta* **1977**, *46*, 1. (d) Ziegler, T.; Rauk, A. *Inorg. Chem.* **1979**, *18*, 1558.
(23) (a) de Jong, G. Th.; Solà, M.; Visscher, L.; Bickelhaupt, F. M. *J. Chem. Phys.* **2004**, *121*, 9982. (b) de Jong, G. Th.; Geerke, D. P.; Diefenbach, A.; Bickelhaupt, F. M. *Chem. Phys.* **2005**, *313*, 261.
(24) de Jong, G. Th.; Geerke, D. P.; Diefenbach, A.; Solà, M.; Bickelhaupt, F. M. *J. Comput. Chem.* **2005**, *26*, 1006.
(25) de Jong, G. Th.; Bickelhaupt, F. M. *J. Phys. Chem. A* **2005**, *109*, 9685.
(26) de Jong, G. Th.; Bickelhaupt, F. M. *J. Chem. Theory Comput.* **2006**, *2*, 322.

imaginary frequency was analyzed to ensure that the correct transition state was found. The steps involving the addition of one acetylene or acetonitrile molecule to the Rh complex have been considered barrierless when the total energy increased in a sequence of constrained geometry optimizations during which the distance between rhodium and the middle point of the triple bond of the unsaturated reactant was kept frozen and progressively elongated. Moreover, spontaneous addition occurred with full geometry optimization starting from one acetylene/acetonitrile molecule and the rhodium complex at large mutual separation.

Several crystallographic structures containing the CpRh fragment were taken from the Cambridge Structural Database, and their relevant geometric parameters (distance between rhodium and the centroid of the Cp ring Q, metal slippage Δ, folding angle of the Cp ring)[27] were considered as an experimental benchmark for the computed structures, since the proposed intermediates have never been crystallographically characterized. The results are included in the Supporting Information.

Gibbs free energies at 298.15 K and 1 atm (ΔG_{298}) were calculated from electronic bond energies (ΔE) and our frequency computations using standard statistical-mechanics relationships for an ideal gas.

2.2. Solvent Effects. Solvent effects in toluene and acetonitrile have been estimated using the conductor-like screening model (COSMO),[16] as implemented in the ADF program.[28] We have used a solvent-excluding surface with an effective radius for toluene of 2.53 Å and acetonitrile of 1.967 Å, derived from the macroscopic density, molecular mass, and a relative dielectric constant of 0.866 g/mL, 92.14 g/mol, and 2.379 and 0.786 g/mL, 41.05 g/mol, and 36.64, respectively. The empirical parameter in the scaling function in the COSMO equation was chosen as 0.0. The radii of the atoms were taken to be MM3 radii,[29] divided by 1.2, giving 1.350 Å for H, 1.700 Å for C, 1.608 Å for N, 1.517 Å for O, and 1.950 Å for Rh (see also ref 30).

2.3. Bond Analysis. To arrive at a better understanding of the nature of selected complexes, an energy decomposition analysis has been carried out.[22] In this analysis, the total binding energy, ΔE, between two molecular fragments of a species is made up of two major components (eq 1):

$$\Delta E = \Delta E_{\text{prep}} + \Delta E_{\text{int}} \quad (1)$$

In this formula, the preparation energy, ΔE_{prep}, is the amount of energy required to deform the individual (isolated) fragments from their equilibrium structure to the geometry that they acquire in the overall molecule. The interaction energy, ΔE_{int}, corresponds to the actual energy change when these geometrically deformed fragments are combined to form the overall complex. It is analyzed in the framework of the Kohn−Sham molecular orbital (MO) model using a quantitative decomposition of the bond into electrostatic interaction, Pauli repulsion (or exchange repulsion or overlap repulsion), and (attractive) orbital interactions (eq 2).[22]

$$\Delta E_{\text{int}} = \Delta V_{\text{elstat}} + \Delta E_{\text{Pauli}} + \Delta E_{\text{oi}} \quad (2)$$

The term ΔV_{elstat} corresponds to the classical electrostatic interaction between the unperturbed charge distributions of the deformed fragments that adopt their positions in the overall molecule and is usually attractive. The Pauli repulsion term, ΔE_{Pauli}, comprises the destabilizing interactions between occupied orbitals and is responsible for the steric repulsion. This repulsion is caused by the fact that two electrons with the same spin cannot occupy the same region in space. The orbital interaction, ΔE_{oi}, in any MO model, and therefore also in Kohn−Sham theory, accounts for electron-pair bonding,[22a,b] charge transfer (i.e., donor−acceptor interactions between occupied orbitals on one moiety with unoccupied orbitals of the other, including the HOMO−LUMO interactions), and polarization (empty−occupied orbital mixing on one fragment due to the presence of another fragment). In the bond energy decomposition, open-shell fragments are treated with the spin-unrestricted formalism, but, for technical (not fundamental) reasons, spin-polarization is not included. This error causes an electron-pair bond to become on the order of a few kcal/mol too strong. To facilitate a straightforward comparison, the results of the bond energy decomposition were scaled to match exactly the (more accurate) regular bond energies. The orbital interaction energy can be further decomposed into the contributions from each irreducible representation Γ of the interacting system using the extended transition state (ETS) scheme developed by Ziegler and Rauk.[22c,d]

3. Results and Discussion

Mechanism of CpRh-Catalyzed Acetylene Cyclotrimerization. The possible pathways leading to the CpRh-catalyzed arene formation are shown in Scheme 2. Regardless the type of metal, it is established that, after a pair of stepwise ligand substitution, resulting in the coordination of two alkyne molecules to the metal center (Scheme 2, cycle *I*, complex **1**), a metallacycle **2** is formed by oxidative coupling of the two alkyne ligands. Two resonance structures can be envisaged for the metallacycle, i.e., the metallacyclopentadiene (represented in Scheme 2), analogous to the predicted species $CpCo(C_4H_4)$,[7] or a metallacyclopentatriene complex having a biscarbene structure, respectively, as predicted for $CpRuCl(C_4H_4)$.[10] By reductive elimination, **2** can be converted into the very stable η^4-cyclobutadiene complex **6**, which is a thermodynamic trap of the catalytic cycle.[31] Instead, the coordination of a third alkyne molecule to the metal center leads to the formation of complex **3**, which is converted into **4** either by direct cycloaddition or by insertion and subsequent reductive elimination, passing through the intermediate metallacycloheptatriene **3′**, as proposed by Schore.[32] Alternatively, on the basis of the experimental results of Booth and co-workers,[33] a nucleophilic ligand L of the catalyst precursor might remain bonded to the metal center throughout the catalytic cycle, as shown in Scheme 2, cycle *II*. The metallacycle **2-L** is an 18-electron complex. Two possible mechanisms might be outlined: (i) The slippage of the η^5-Cp ring to an η^3 coordination mode opens a free site at the metal, so that an alkyne molecule can coordinate. In this case the arene construction occurs by subsequent intramolecular cycloaddition, leading to **4-L**. (ii) The direct Diels−Alder-like cycloaddition between the metallacycle and an alkyne molecule gives the metallanorbornadiene intermediate **4′-L**, which is converted into **4-L** by migration of the L_nRhL' group to an η^2 coordination position.

The energy profile of the CpRh-catalyzed acetylene cyclotrimerization is presented in Scheme 3; the relevant geometric

(27) The slippage parameter Δ is defined as Δ = 1/2[(M−C1a + M−C3a) − (M−C1+ M−C3)] where M−C1a and M−C3a are the longest distances between M and two adjacent C atoms of the Cp ring and M−C1 and M−C3 are the distances between M and the C atoms adjacent to C1a and C3a, respectively; in indenyl complexes C1a and C3a are the hinge C atoms.

(28) Pye, C. C.; Ziegler, T. *Theor. Chem. Acc.* **1999**, *101*, 396.
(29) Allinger, N. L.; Zhou, X.; Bergsma, J. *J. Mol. Struct. (THEOCHEM)* **1994**, *312*, 69.
(30) Bon, R. S.; van Vliet, B.; Sprenkels, N. E.; Schmitz, R. F.; de Kanter, F. J. J.; Stevens, Chr. V.; Swart, M.; Bickelhaupt, F. M.; Groen, M. B.; Orru, R. V. A. *J. Org. Chem.* **2005**, *70*, 3542.
(31) Veiros, L. F.; Dazinger, G.; Kirchner, K.; Calhorda, M. J.; Schmid, R. *Chem.−Eur. J.* **2004**, *10*, 5860.
(32) Schore, N. E. *Chem. Rev.* **1988**, *88*, 1081.
(33) Abdulla, K.; Booth, B. L.; Stacey, C. *J. Organomet. Chem.* **1985**, *293*, 103.

Scheme 2. Possible Pathways of CpRh-Catalyzed Acetylene Cyclotrimerization to Benzene

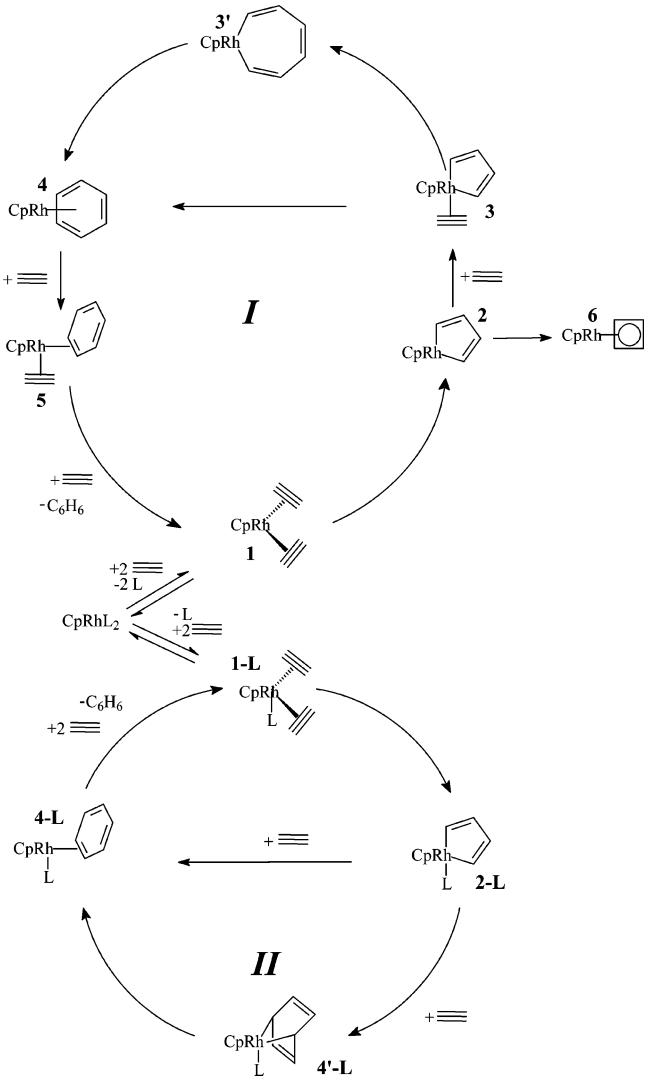

parameters of the intermediates and transition states are shown in Figure 1. The complex $[(\eta^5\text{-}C_5H_5)Rh(C_2H_2)_2]$ (**A1**) is generated by replacing thermally or photochemically the ancillary ligands L of a suitable catalyst precursor of general formula $[(\eta^5\text{-}C_5H_5)RhL_2]$($L = C_2H_4$, PH_3, CO; L_2 = COD).

Experimental evidence and theoretical studies have demonstrated that the mechanism of the reactions of substitution of the ancillary ligands in half-sandwich CpM derivatives might be dissociative or associative, depending on the nature of the metal, on the substituents on the Cp ring, and on the electrophilicity of the ancillary ligands.[34] Associative mechanisms are possible only if a haptotropic shift from η^5 to at least a η^3 bonding mode occurs and opens a coordination site at the metal center. In $CpRhL_2$ complexes it has been experimentally observed that (i) olefins are displaced in mild conditions, while carbonyl groups require higher thermal energy or photolysis, and (ii) electron-withdrawing substituents on the Cp ring favor an associative mechanism, while electron-donor substituents favor a dissociative mechanism.[34] Since the generation of the catalyst **A1** from the precursor $CpRhL_2$ is not part of the catalytic cycle, this topic is not investigated further in this context, but might deserve deeper scrutiny in future work.

In **A1** the acetylene ligands, which lie almost parallel to the Cp plane, are weakly bound to the metal center, with the C−C bond length of 1.26 Å, which is elongated only by 0.05 Å relative to free acetylene (1.21 Å).

By oxidative coupling of the two alkyne ligands of **A1** the rhodacycle **A2** is formed (Figure 1). According to the calculated structure, the cycle is close to a metallacyclopentadiene, as found for the cobalt analogous complex.[7] The $C_\alpha-C_\beta$ and $C_\beta-C_{\beta'}$ distances of 1.35 and 1.48 Å well match with ethylene double-bond length (1.32 Å) and the length of a σ bond between two sp^2 carbon atoms (1.50 Å). The C−Rh distance of 2.06 Å is in good agreement with average crystallographic C−Rh σ bond lengths (2.01 Å). The rhodacycle shows a bent conformation; that is, it is tilted from the axis defined by the rhodium atom and the centroid of the Cp ring (Q) by 32°. An appreciable fold angle of 5° is also present. Recently an unusual nontilted and planar rhodacycle has been predicted,[31] whose formation from **A1** is symmetry forbidden.[35] This prompted us to further investigate the intermediate **A2**. At the employed level of theory an orthogonal rhodacycle **A2′** is found as a transition state between two equivalent tilted **A2** structures (Figure 2). The interconversion barrier is 6.8 kcal/mol. No minimum energy orthogonal rhodacycle has been located on the PES at the employed level of theory.

In order to explain why the conformation of **A2′** is energetically unfavored with respect to **A2**, a bond energy decomposition analysis was performed. **A2** and **A2′** have been built from the two fragments CpRh (**Fg1**) and C_4H_4 (**Fg2**), and C_s symmetry has been imposed. To facilitate the analysis, the C_4H_4 plane of **A2′** has been slightly rotated, making the mirror plane perpendicular to the C_4H_4 plane. This rotation causes an increase of 0.9 kcal/mol. The most important fragment orbitals of **A2** and **A2′** are given in Scheme 4. The CpRh fragment, **Fg1**, has a ground state with one electron in a 4d-derived orbital of A″ symmetry (HOMO−1) and one electron in a 4d-derived orbital of A′ symmetry (HOMO); these orbitals are indicated in Scheme 4 on the metal fragment. The ground state of the CpRh fragment also corresponds to its valence state in the overall complex with the C_4H_4 fragment. In the C_4H_4 fragment, an electron from the HOMO−1 (A′ symmetry) has to be excited to the LUMO (A″ symmetry) to turn this fragment into the appropriate valence state for bonding with the metal fragment.

Results of our quantitative decomposition analysis are given in Table 1. Most striking is the almost zero overlap for the HOMO of the metal fragment with the HOMO−1 of the C_4H_4 fragment, $\langle$HOMO|HOMO−1$\rangle$, in A′ symmetry for **A2**. This weak overlap results in a much lower orbital interaction in A′ symmetry, $\Delta E_{oi}(A')$, for the orthogonal **A2′** than for the tilted **A2** conformation. This ineffective overlap for **A2′** is depicted in Scheme 4, where it is clearly seen that the "p" orbitals of C_4H_4 overlap with both the positive and negative lobe of the "d" orbital of the metal, while the bent structure of **A2** overlaps only with a positive lobe of the "d" orbital of the metal.

The conversion of **A1** into **A2** is exothermic by 15.4 kcal/mol, while the activation barrier is 12.7 kcal/mol. These values nicely compare to those found for the CpCo analogue, i.e., 13.1 and 12.8 kcal/mol, respectively.[7] In contrast the conversion of

(34) (a) Ziegler, T.; Tschinke, V.; Fan, L.; Becke, A. D. *J. Am. Chem. Soc.* **1989**, *111*, 9177. (b) Basolo, F. *Coord. Chem. Rev.* **1982**, *43*, 7. (c) Janowicz, A. H.; Bryndza, H. E.; Bergman, R. G. *J. Am. Chem. Soc.* **1981**, *103*, 1516. (d) Cramer, R.; Seiwell, L. P. *J. Organomet. Chem.* **1975**, *92*, 245. (e) Schuster-Woldan, H. G.; Basolo, F. *J. Am. Chem. Soc.* **1966**, *88*, 1657.

(35) Wakatsuki, Y.; Nomura, O.; Kitaura, K.; Morokuma, K.; Yamazaki, H. *J. Am. Chem. Soc.* **1983**, *105*, 1907.

Scheme 3. Energy Profile of the Cyclization of Three Acetylenes by the CpRh Fragment (energies in kcal/mol relative to the bisacetylene complex A1)

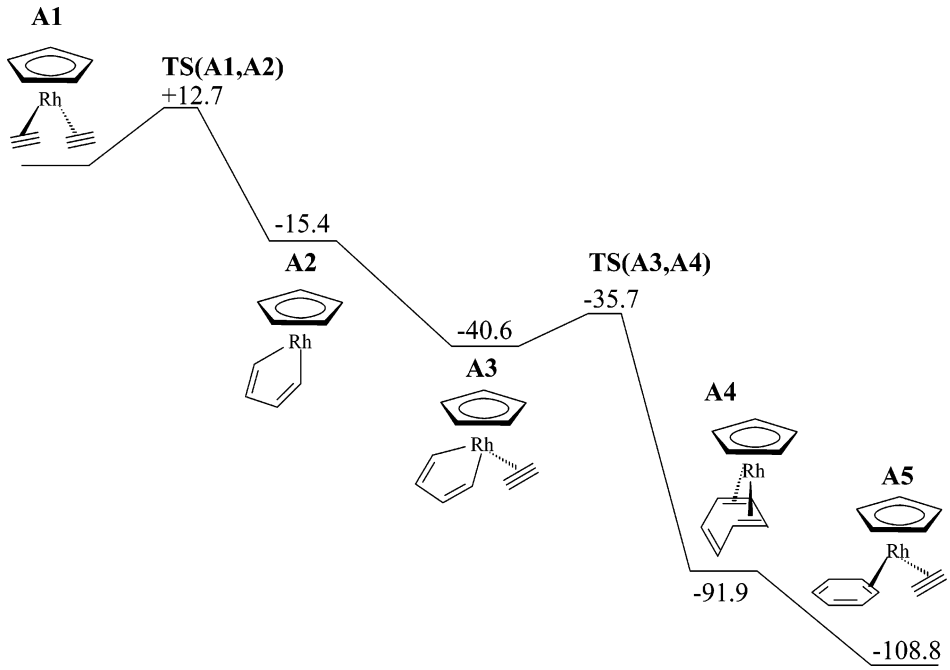

the CpRuCl bisacetylene complex into the peculiar metallacycloheptatriene has a similar activation energy, 13.2 kcal/mol, but the released energy is 38.7 kcal/mol.[10]

In the geometry of the transition state between **A1** and **A2**, denoted **TS(A1,A2)** (Figure 1), a significant shortening of the Rh−C_α bond lengths is observed and the C_β−$C_{\beta'}$ is nearly formed. In contrast, the C_α−C_β bonds are only slightly elongated with respect to **A1**.

Complex **A2** is a coordinatively unsaturated 16-electron species. Thus it may react in facile manner with a third acetylene molecule to form the addition product **A3** (Figure 1); the reaction was found to be barrierless and exothermic by 25.2 kcal/mol. The tilt angle of the metallacycle is 42°, and no folding is observed. Although no symmetry was imposed, both **A2** and **A3** have C_s symmetry. In **A3**, the addition of acetylene to the rhodacycle occurs with the triple bond oriented perpendicular to the Rh−Q axis, an orientation preference resulting from a stronger back-bonding contribution to the rhodium−acetylene bond (C−C−H = 156°), as predicted by others.[36] Interestingly, the coordination of the third acetylene modifies only slightly the carbon−carbon bonds of the rhodacycle and the relevant change is the increase of the tilt angle by 10°. In **A3**, the acetylene C−C bond length elongates to 1.26 Å.

The rearrangement converting **A3** into **A4** is a [4+2] cycloaddition of the coordinated acetylene with the rhodacycle π system. This process has a low activation barrier (4.9 kcal/mol) and is exothermic by 51.3 kcal/mol. The geometry of **TS(A3,A4)** (Figure 1) is very similar to that of **A3**, and C_s symmetry is preserved along the path connecting the initial and final state. Complex **A4** (Figure 1) is characterized by the presence of a six-carbon arene ring coordinated to rhodium in η^4 fashion. This ring exhibits a hinge angle of 37°. In the crystallographic structure of the similar complex [η^4-$C_6(CH_3)_6$]-Rh[(η^5-$C_5(CH_3)_5$] a very similar hinge angle was measured, i.e., 42°.[37] A localized double bond (1.35 Å) is observed in the portion of the ring that is bent away from the metal atom. The axis of this bond is orthogonal to the molecular symmetry plane.

The release of the benzene ring from **A4** occurs after the subsequent stepwise addition of two acetylene molecules to regenerate the catalyst **A1**. The coordination of the first acetylene leads to the formation of the intermediate **A5** (Figure 1), in which the benzene ring is coordinated to rhodium in η^2 fashion. The reaction is exothermic by 16.9 kcal/mol. The geometric features of **A5** nicely compare with those of the complex (η^5-C_5H_5)Rh[$P(CH_3)_3$](η^2-C_6F_6) found in the CSD.[38] Since no transition state connecting **A4** to **A5** was found, the energy barrier of this step is expected to be very low or absent. The six-carbon ring is planar and exhibits in part bond-length alternation in one-half of the arene, but the C−C bonds adjacent to the C−C bond of benzene coordinating to the metal are all similar. The addition of a second acetylene molecule was found to be barrierless and leads to the displacement of the benzene ring and the formation of **A1**; also this final step is exothermic, by 17.0 kcal/mol. The mechanism illustrated in Scheme 3 has numerous analogies to the CpCo-catalyzed mechanism proposed by Albright,[7] but interestingly (i) **A3** has been found in the present study, but no analogous species was located on the PES of the CpCo-catalyzed process, because in the latter the barrier for the addition of acetylene to the metallacycle is too small and the adduct CpCo(C_4H_4)(C_2H_2) collapses directly to CpCo-(η^4-C_6H_6), and (ii) the overall process is slightly more exothermic when CpRh instead of CpCo is employed, i.e., 126 kcal/mol versus some 114 kcal/mol, respectively.

The alternative mechanism proposed by Schore[32] was also investigated (Scheme 2, cycle *I*). Starting from **A3** the insertion of the coordinated acetylene into a Rh−C_α σ bond leads to the formation of the seven-membered-ring rhodacycle **A3′** (Figure 3), which was found to lie 29.2 kcal/mol below **A3** and 22.1 kcal/mol above **A4**. The inspection of the bond lengths of this intermediate suggests that it is a rhodacycloheptatriene that undergoes C−C bond length equalization due to a certain extent of back-donation from the metal into the π system of the organic

(36) Schilling, B. E. R.; Hoffmann, R.; Lichtenberger, D. L. *J. Am. Chem. Soc.* **1979**, *101*, 585.

(37) Bowyer, W. J.; Merkert, J. W.; Geiger, W. E.; Rheingold, A. L. *Organometallics* **1989**, *8*, 191.

(38) Belt, S. T.; Helliwell, M.; Jones, W. D.; Partridge, M. G.; Perutz, R. N. *J. Am. Chem. Soc.* **1993**, *115*, 1429.

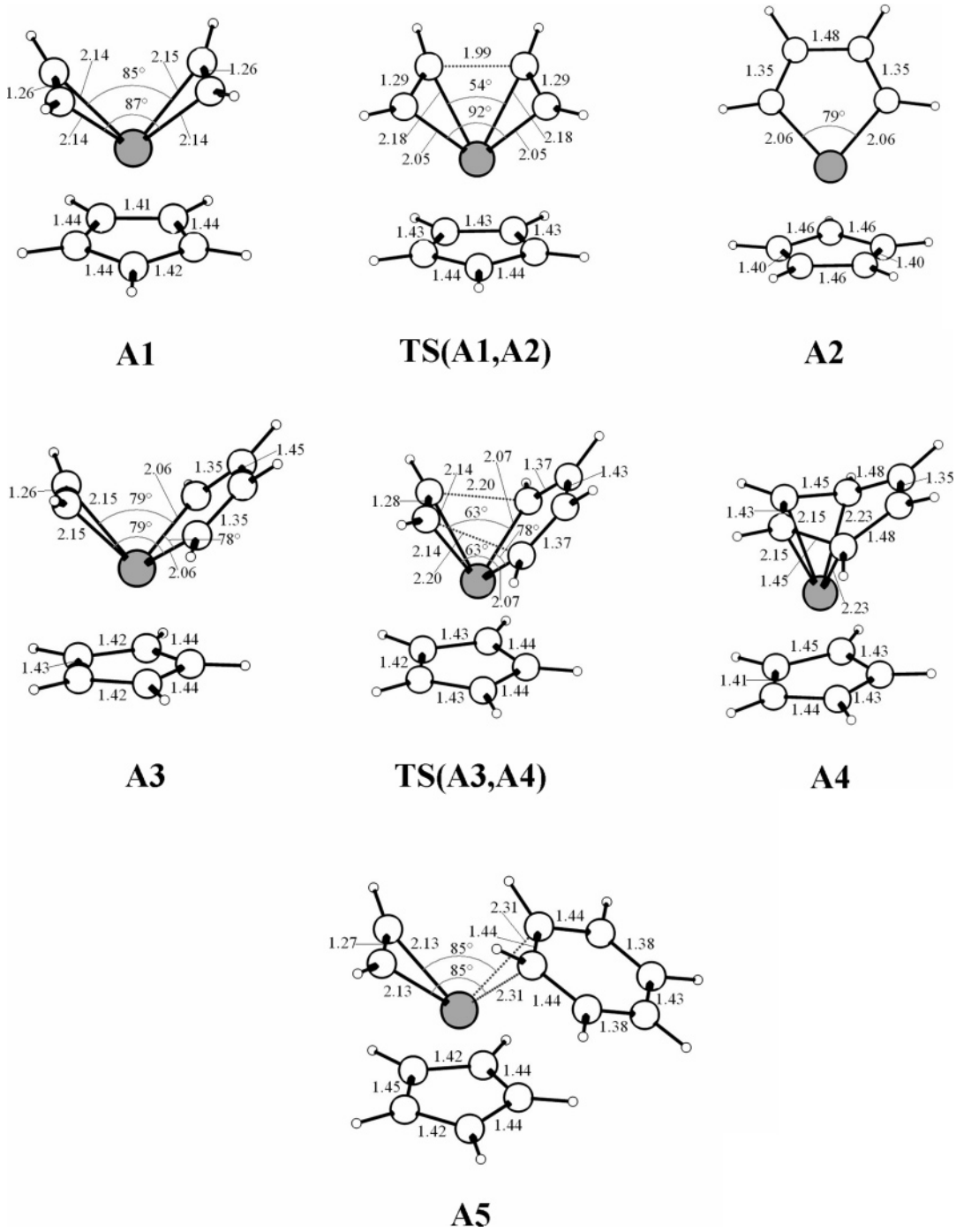

Figure 1. Structures of rhodium species shown in Scheme 3 with selected interatomic distances (Å) and angles (deg).

fragment. Also in the planar cobaltacycloheptatriene located by Koga et al.[9a] on the singlet B3LYP/6-31G** PES, the five C−C distances have almost the same bond lengths, ranging from 1.387 to 1.405 Å, and as explained by the authors, the six π electrons can indeed constitute an aromatic ring through the formally vacant d orbital of the metal.

The transition state connecting **A3** and **A3′** was located 5.5 kcal/mol above **A3**; this barrier is comparable to the energy difference between **A3** and **TS(A3,A4)**. But the reductive elimination, by which **A3′** is converted into **A4**, has a rather high activation energy, i.e., 22.1 kcal/mol, due to the symmetry-forbidden nature of the reaction. **TS(A3,A3′)** (Figure 3) and **TS(A3,A4)** (shown in Figure 1) are structurally similar. In the former a slight asymmetry in the distances between the acetylenic C atoms and the C_α of the rhodacycle and in the angles they form with rhodium is present, 2.18 and 2.22 Å and 62° and 64°. **TS(A3′,A4)** (Figure 3) is quite dissimilar to **A3′**, not only because in the transition-state geometry the seven-membered ring is remarkably bent but also for the strong shortening of the interatomic distance between the C_α atoms (from 2.91 Å to 2.08 Å) and the presence of a distinct bond length alternation. It is worth noticing that no reaction path connecting the Co analogues of **A3** and **A4** through the planar cobaltacycloheptatriene was found.[9] In contrast, in the CpRuCl-catalyzed acetylene cyclotrimerization, the predicted puckered seven-membered ruthenacycle converts very easily into the last intermediate with an η^2-coordinated benzene (the activation energy is less than 2 kcal/mol).[10] **A3′** is more resistant to a reductive elimination because of its nearly C_s symmetry.

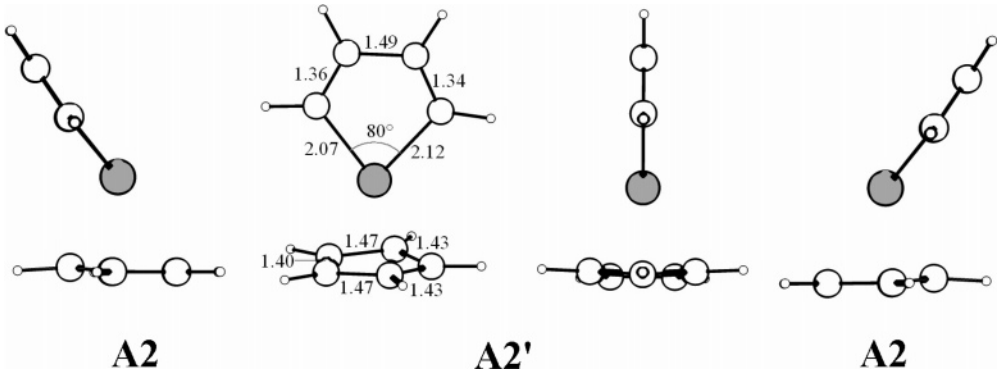

Figure 2. Structures of rhodium metallacycles **A2** and **A2′** with selected interatomic distances (Å) and angles (deg).

Scheme 4. Schematic Representation of the Most Important Orbital Overlaps (in A′ and A″ symmetry) between CpRh (Fg1) and C_4H_4 (Fg2) in the Tilted A2 and Orthogonal A2′ Conformations

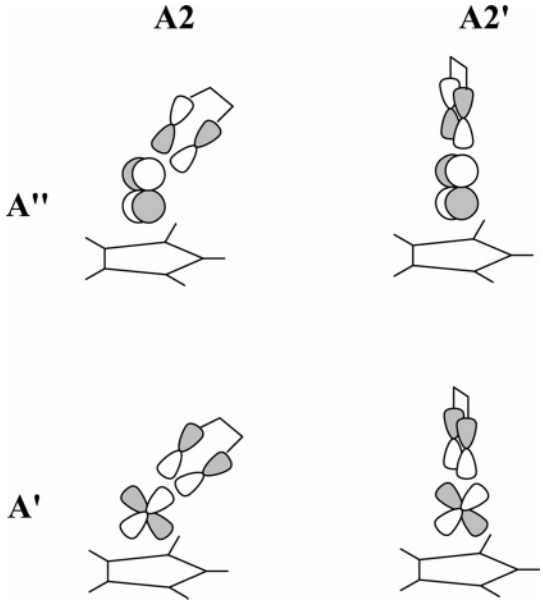

Finally we have investigated a possible mechanism starting from the catalyst [(η^1-C_5H_5)Rh(C_2H_2)$_2$(CO)] (**A1-CO**) (Figure 4), which is formed from the precursor [(η^5-C_5H_5)Rh(CO)L] by sequential replacement of L with an acetylene molecule and addition of the second acetylene accompanied by the haptotropic shift $\eta^5 \rightarrow \eta^1$. No η^3 intermediate was located at the employed level of theory. The oxidative coupling of the alkyne ligands has an activation energy comparable to the barrier calculated for the conversion of **A1** to **A2**, i.e., 12.9 kcal/mol, but the formation of the metallacycle [(η^5-C_5H_5)-Rh(C_4H_4)(CO)] (**A2-CO**) is highly exothermic (60.6 kcal/mol) and involves the haptotropic shift $\eta^1 \rightarrow \eta^5$. **A2-CO** (Figure 4) is an 18-electron intermediate, thus possessing low reactivity. Upon coordination of the third acetylene molecule, **A3-CO** is formed, which is again characterized by η^1 hapticity (Figure 4).

This reaction is highly endothermic (32.3 kcal/mol) and is not likely to occur. Alternatively, a direct Diels−Alder-like addition of acetylene to the π system of the metallacycle was attempted, but this led to a highly strained polycyclic intermediate. No metallanorbornadiene intermediate was found, analogous to that elegantly excluded by Albright for the CpCo-catalyzed mechanism.[7] These results clearly indicate that if the vacant coordination site of the 16-electron metallacycle is

Table 1. Energy Decomposition (in kcal/mol) for the Interaction between CpRh (Fg1) and C_4H_4 (Fg2) in the Tilted A2 and Orthogonal A2′ Conformations[a]

	A2	A2′
ΔE	−90.0	−82.3
ΔE_{prep}	57.0	55.8
ΔE_{int}	−147.1	−138.1
ΔE_{Pauli}	232.8	180.8
ΔV_{elst}	−179.1	−139.8
ΔE_{oi}	−200.8	−179.1
$\Delta E_{oi}(A')$	−100.1	−86.1
$\Delta E_{oi}(A'')$	−100.7	−93.1
fragment orbital overlap		
⟨HOMO|HOMO−1⟩	0.228	0.015
⟨HOMO−1|LUMO⟩	0.284	0.314

[a] Computed at BLYP/TZ2P. See Scheme 4 for an illustration of selected fragment orbital overlaps.

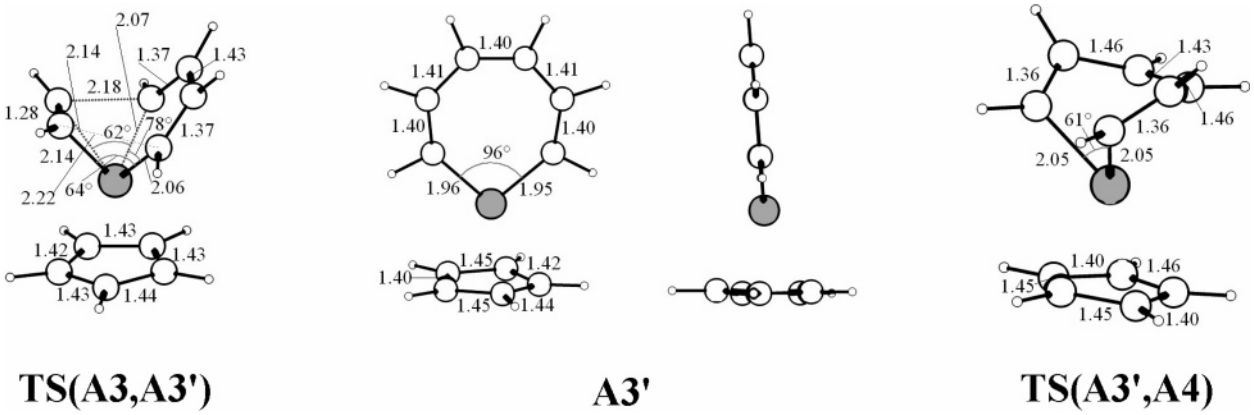

Figure 3. Structures of **TS(A3,A3′)**, **A3′** (front and side view), and **TS(A3′,A4)** with selected interatomic distances (Å) and angles (deg).

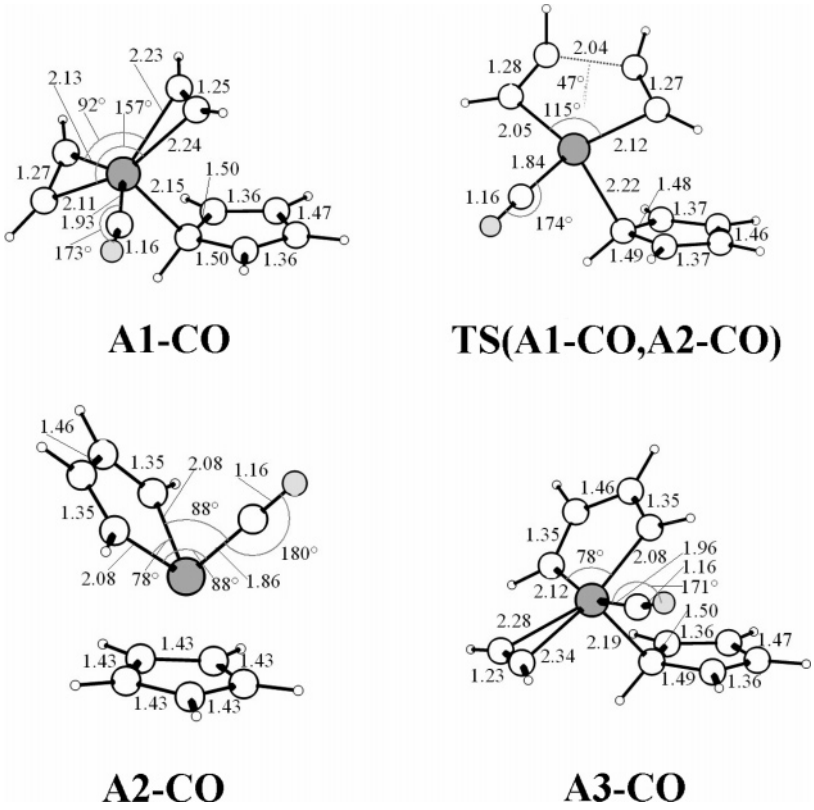

Figure 4. Structures of **A1-CO**, **TS(A1-CO, A2-CO), A2-CO**, and **A3-CO** with selected interatomic distances (Å) and angles (deg).

blocked by an ancillary ligand of the catalyst precursor that never dissociated or reentered in the catalytic cycle (this might be the case of strongly nucleophilic ligands like phosphines), the mechanism is interrupted, as found for the CpCo-catalyzed mechanism.[7]

Mechanism of CpRh-Catalyzed Acetylene/Acetonitrile Cocyclization. As postulated for the mechanism of acetylene self-trimerization to benzene, the CpRh-catalyzed synthesis of 2-methylpyridine from acetylene and acetonitrile initiates with the formation of a rhodacycle by oxidative coupling of the two alkyne ligands of the catalyst. In the presence of acetonitrile the equilibrium shown in eq 3 occurs, but the computed Gibbs free energy variation of the reaction ($\Delta G_{298} = +11.5$ kcal/mol) is in favor of the reactants.

$$RhCp(C_2H_2)_2 + CH_3CN \rightleftarrows RhCp(C_2H_2)(CH_3CN) + C_2H_2 \quad (3)$$

This is in agreement with the experimental findings and leads us to the conclusion that the formation of bisacetylene species is favored also in cocyclization processes, as it has been established also for CpCo-catalyzed cocyclization of acetylene/ethylene[8] and for the CpRuCl-catalyzed cocyclization of acetylene/nitriles.[12] But acetylene and acetonitrile compete also to coordinate to the 16-electron metallacycle in the second stage of the mechanism and, in this case, the Gibbs free energy variation of the reaction of eq 4 is in favor of the products ($\Delta G_{298} = -12.4$ kcal/mol).

$$RhCp(C_4H_4)(CH_3CN) + C_2H_2 \rightleftarrows RhCp(C_4H_4)(C_2H_2) + CH_3CN \quad (4)$$

This explains why good yields of pyridine are obtained only with an excess of nitriles. While an excess of nitrile will increasingly favor eq 3 relative to eq 4 and the energy barriers for the oxidative coupling steps are similar, regardless of whether two alkynes or one alkyne and one nitrile are coupled, the rhodacycle was predicted to be ~10 kcal/mol more stable than the azametallacycle.[11] Therefore we have explored only the pathways leading to the formation of 2-methylpyridine involving the rhodacycle (Scheme 5).

The coordination of the acetonitrile molecule may occur "side-on", $\mathbf{3}_{\mathbf{side\text{-}on}}$, i.e., through the C≡N π system, or "end-on", $\mathbf{3}_{\mathbf{end\text{-}on}}$, i.e., by forming a Rh−N σ bond. The latter bonding mode is common and is found in most of the crystal structures included in the CSD, although an example of the former was also reported.[39] Like in the mechanism proposed for acetylene self-trimerization, the unsaturated molecule can add directly to the π system of the rhodacycle or insert in the Rh−C_α σ bond to generate a seven-membered azametallacycle ($\mathbf{3'}_{\mathbf{pyr}}$), which is subsequently converted by reductive elimination into $\mathbf{4}_{\mathbf{pyr}}$, an intermediate in which the pyridine ring is already formed, but still coordinated to the metal center.

The energy profile of the CpRh-catalyzed cotrimerization of acetylene and acetonitrile is shown in Scheme 6; the relevant geometric parameters of the intermediates and transition states are shown in Figure 5.

The "side-on" coordination of CH_3CN (complex **B3**, Figure 5) does not essentially perturb the geometry of the metallacycle, but is accompanied by an increase of the tilt angle to 45°. This step is barrierless and exothermic by 13.4 kcal/mol. In **B3** the Rh−C_{CN} distance is shorter than the Rh−N distance, i.e., 2.18 versus 2.21 Å, in anticipation that **B3** is converted into the bicyclic intermediate **B4** (Figure 5) through the formation of a σ bond between C_{CN} and C_α of the rhodacycle. This step is slightly endothermic (1.2 kcal/mol) and has an activation energy of 11.1 kcal/mol. Interestingly, a similar bicyclic intermediate was located on the PES of CpRuCl-catalyzed trimerizations.

(39) Albano, V. G.; Braga, D.; Chini, P.; Martinengo, S.; Strumolo, D. *Eur. Cryst. Meet.* **1980**, *6*, 71.

Scheme 5. Possible Pathways of CpRh-Catalyzed Acetylene/Acetonitrile Cocyclization to 2-Methylpyridine

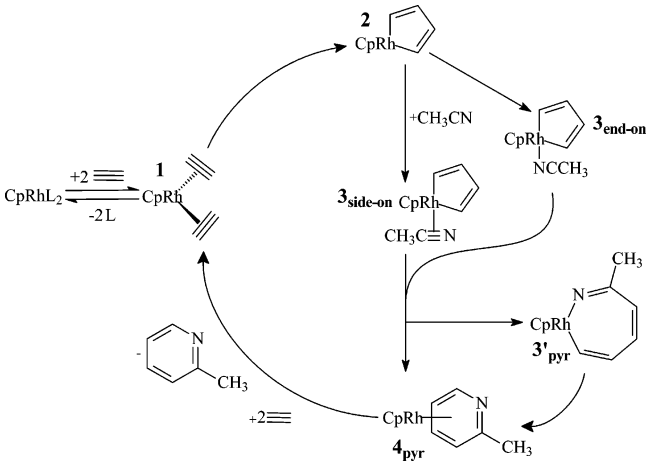

The "end-on" bonding mode of CH_3CN to **B2** leads to the formation of **B3′** (Figure 6), which is 8.3 kcal/mol more stable than **B3**. The tilt angle of the metallacycle in **B3′** is 41°. Dazinger et al.[11] postulate an intermediate structurally analogous to **B4** for the cocyclization of acetylene and HCN catalyzed by the CpRh fragment. We have found that the formation of **B4** can occur also from **B3′**. The transition state (**TS(B3′,B4)**, Figure 6) was located 17.6 kcal/mol above **B3′**, and the reaction is endothermic by 9.6 kcal/mol. In the CpRuCl-catalyzed mechanism, the end-on coordination of acetonitrile leads to a complex that is also more stable than the side-on isomer (6.9 kcal/mol), but only the latter was connected to the subsequent steps of the cycle.[11] In the CpRh-catalyzed mechanism both **B3** and **B3′** are likely populated states and, although the path through **B3′** is energetically favored, the path through **B3** is kinetically favored. **B3** is a more reactive intermediate, as discussed also by Dazinger, who revisited the bonding mode of a nitrile to a metal center.[11] It is worth noting that Ingrosso and co-workers invoked a "side-on" intermediate to interpret the observed regioselectivity, which depends on the nature of the alkyl group R of the nitrile reactant of general formula R−CN.[17a] On the basis of our results, the steric encumbrance of R may influence both the transition states **TS(B3,B4)** and **TS(B3′,B4)**, thus affecting the regioselectivity.

By initial elongation of the $C_{CN}-C_\alpha$ distance and progressive shortening of the $N-C_\alpha$ distance **B4** is converted into **TS(B4,B5)**, which subsequently rearranges into **B5** (Figure 5), in which a bent pyridine ring is coordinated to the metal through N and three C atoms. The energy barrier is 9.9 kcal/mol, and 20.1 kcal/mol are released. Alternatively, if only the distance between C_α and Rh elongates, **B4** transforms into **TS(B4,B5′)**, which subsequently evolves into the strongly bent seven-membered rhodacycle **B5′** (Figure 7). This step is energetically favored with respect to the conversion **B4**−**B5** since it has a lower activation energy, i.e., 8.3 kcal/mol, but is exothermic only by 10.4 kcal/mol. However, if **B5′** is included in the mechanism, a subsequent reductive elimination step must be conceived. Such rearrangement has an activation energy of 14.3 kcal/mol and is exothermic by 9.7 kcal/mol. On the basis of the energetics the direct conversion of **B4** into **B5** is clearly favored. **B5′** is very dissimilar from **A3′**: the cycle is strongly bent and exhibits bond length alternation.

On the B3LYP/SDD,6-31G** PES Dazinger et al.[11] find a slightly different path connecting **B3** to **B5**; that is, an intermediate is located in which the 18-electron rule at the metal is satisfied with one Rh−C and one Rh−N single bonds and π bonding of the internal olefinic double bond of the azarhodacycle. The mechanism involves a weakly endothermic step

Scheme 6. Energy Profile of the Cocyclization of Two Acetylenes with Acetonitrile by CpRh Fragment (energies in kcal/mol relative to the bisacetylene complex B1)

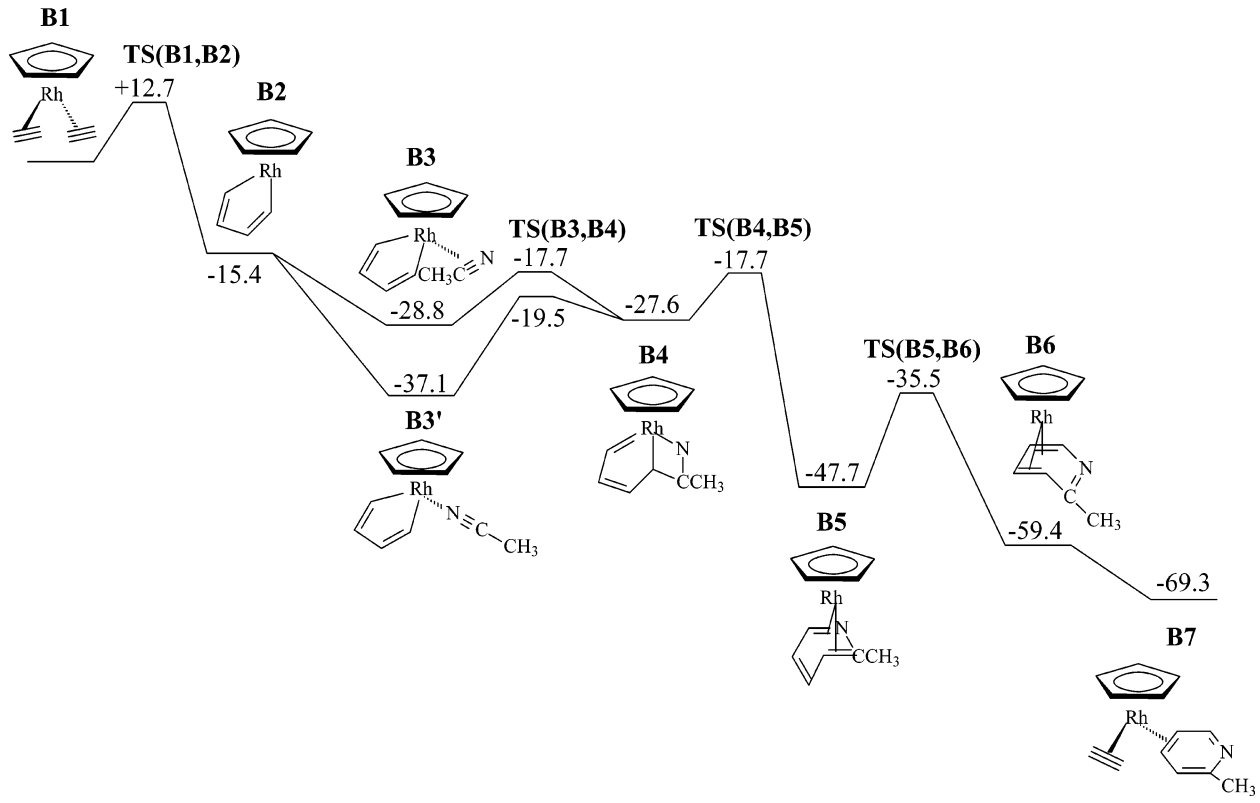

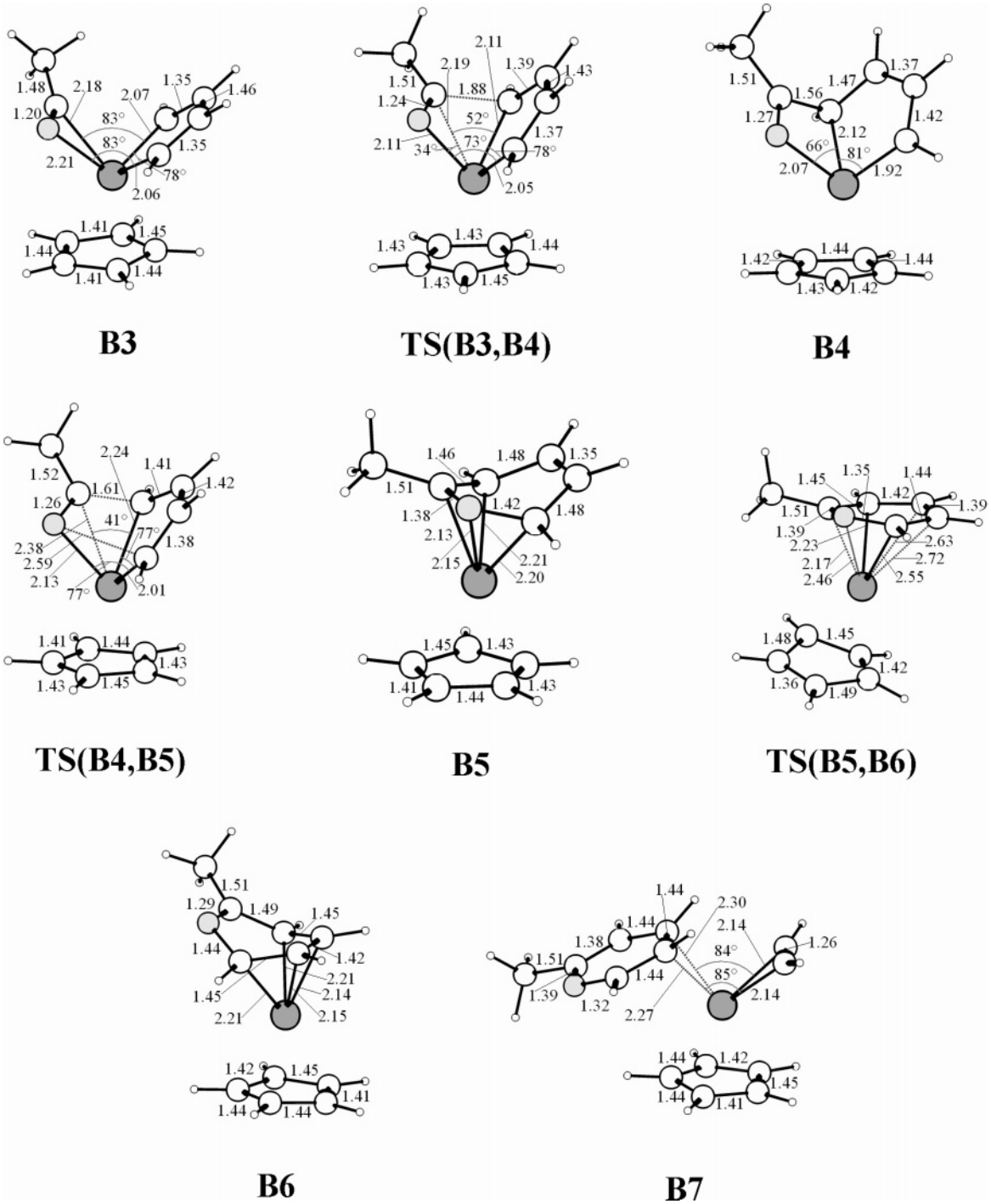

Figure 5. Structures of rhodium species shown in Scheme 6 with selected interatomic distances (Å) and angles (deg).

(activation energy of 6.4 kcal/mol and $\Delta E = +0.6$ kcal/mol) and a subsequent exothermic step (activation energy of 6.9 kcal/mol and $\Delta E = -31.3$ kcal/mol). The last stage in this mechanism is the formation of **B5**, from which the pyridine is released and the catalyst exothermically regenerated ($\Delta E = -26.0$ kcal/mol).

Before the release of 2-methylpyridine occurs, a further rearrangement of **B5** must be included, i.e., a hapticity variation of the Rh−pyridine moiety that leads to **B6** (Figure 5). The activation energy is 12.2 kcal/mol, and this stage is exothermic by 11.7 kcal/mol. In **B6** the metal is coordinated to the bent pyridine ring in η^4 fashion through four carbon atoms.

The stepwise addition of two acetylene molecules regenerates the catalyst and releases 9.9 kcal/mol concomitantly with the formation of **B7** (Figure 5) and 17.0 kcal/mol when 2-methylpyridine is finally released. **B7** is characterized by the planar 2-methylpyridine moiety coordinated in η^2 fashion to rhodium and shows structural features similar to **A5**. The addition of an acetylene molecule to **B5′** was also attempted, and it led to the stable complex **B8** (Figure 8). This is in contrast with the mechanistic stage postulated for the CpRuCl seven-membered ring complex, which, by coordination of an unsaturated molecule to Ru, is converted into a reactive intermediate with the arene coordinated to the metal in η^2 fashion.[10,40] The formation of **B8** is slightly endothermic (3.0 kcal/mol). The coordination of acetylene weakens the bonds Rh−C_α and Rh−N, but, since the angle C_α−Rh−N is essentially unchanged (88°), the closure of the pyridine ring is prevented.

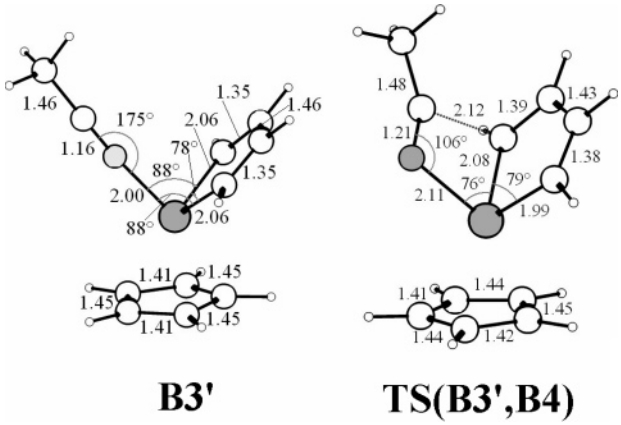

Figure 6. Structures of **B3′** and **TS(B3′,B4)** with selected interatomic distances (Å) and angles (deg).

Alternatively, the formation of **B8′** from **B5** can be conceived as occurring via addition of an acetylene molecule and the formation of a Rh−N σ bond. **B8′** (Figure 8) lies 31.9 kcal/mol below **B5** and is also energetically favored relative to **B7** by 10.3 kcal/mol.

Mechanism of IndRh-Catalyzed Acetylene Cyclotrimerization. Modifications of the Cp ligand influence the catalyst's efficiency and selectivity. In particular, it has been observed that in the presence of an electron-withdrawing substituent the reactivity at low temperatures is reduced, but the chemo- and regioselectivity increase and vice versa.[17b] An alternative variation is to introduce a larger π aromatic ligand, thus inducing a metal hapticity variation toward a more allylic coordination. The first choice is the aromatic indenyl ligand. As first noted by Green,[41] the η^5 indenyl ligand undergoes a facile slippage to an η^3 indenyl ligand[42] and should catalyze cyclotrimerization reactions by a similar mechanism to that proposed for the CpRh complex. The generation of the active catalyst from the indenyl catalyst precursor, i.e., the substitution of the ancillary ligands, occurs certainly faster in indenyl complexes ("indenyl effect")[19] than in cyclopentadienyl analogues. Ingrosso reports lower pyridine yields for the cocyclization of 1-hexyne and propionitrile when the Ind catalyst is used instead of the Cp analogue and longer reaction times, but higher regio- and chemoselectivity.[17a]

As illustrated in Scheme 7, the energy profile of the acetylene cyclotrimerization catalyzed by the IndRh fragment closely resembles that shown in Scheme 3 for the CpRh fragment.

The presence of the benzene moiety fused to the Cp ring has important steric effects, which can explain the higher selectivity of this catalyst. In the bisacetylene indenyl complex **C1** (Figure 9), the acetylene ligands are tilted off from the plane parallel to the aromatic ring, in an arrangement apparently favorable to the formation of a metallacycle bent back toward the benzene ring. Instead the formation of the rhodacycle is accompanied by a rotation of the group Rh(C_4H_4), and the initial C_s symmetry is completely lost (**C2**, Figure 9). The metallacycle is tilted by 34° and exhibits a moderate folding angle (5°). The interatomic distances and angles are almost identical to those measured in **A2** (Figure 2). The transition state **TS(C1,C2)**, which lies 15.2 kcal/mol above the initial bisacetylene complex, is structurally very similar to **C1**; the distance between the metal and the centroid of the Cp ring is slightly increased by 0.03 Å, and the folding angle is reduced from 10° to 7°. The formation of **C2** is exothermic by 18.6 kcal/mol.

It is worth noting that the metal slippage of **C2** is much more pronounced than **A2** (the metal slippage parameters Δ are 0.28 and 0.064 Å, respectively), and this should favor the coordination of the third acetylene molecule. Nevertheless the charge of the metal is not appreciably different in the two species, and no evidence of an η^3 indenyl intermediate in this path of cycloaddition has been found. The barrierless coordination of the third acetylene leads to the formation of **C3**, with the release of 20.7 kcal/mol. Upon the subsequent addition of the coordinated alkyne to the π system of the rhodacycle, which has an activation energy of 6.9 kcal/mol, the complex **C4** is formed, which is characterized by nearly C_s symmetry. Although the energy required for the formation of **C4** is slightly higher than that required for **A4**, this step is also more exothermic, i.e., 55.8 versus 51.3 kcal/mol.

Finally the catalyst is regenerated, passing through the intermediate **C5**, whose formation releases 5.5 kcal/mol; the energy released in the last step is 26.6 kcal/mol. The IndRh-catalyzed acetylene self-trimerization is thermodynamically less favorable than the CpRh-catalyzed process: no "indenyl effect" is observed, and the poorer performance may be due to the fact that the indenyl group is a less efficient donor ligand and more sterically hindered than the cyclopentadienyl ligand.

We have also explored if the mechanism suggested by Booth, i.e., with an ancillary ligand of the catalyst precursor bound to rhodium throughout the cycle, might work for the IndRh catalyst. In Figure 10 the located intermediates **C1-CO, C2-CO**, and **C3-CO** are shown, together with the transition-state geometry **TS(C1-CO,C2-CO)**. The energy barrier relative to the metallacycle formation, which is accompanied by the haptotropic shift $\eta^1 \rightarrow \eta^5$, is 13.6 kcal/mol, and 44.5 kcal/mol are released. The addition of the third acetylene molecule generates the η^1 intermediate **C3-CO**, but this step is endothermic (16.8 kcal/mol), and this led us to exclude this path. Notably the energy required to form **C3-CO** is almost half of the energy required to generate the analogous **A3-CO**, due to the major flexibility of the indenyl ligand to undergo haptotropic shifts.

Solvent Effects on the Catalytic Cycles. The solvent effects on the energetics have been explored by using the COSMO model (see Computational Details). Alkyne self-trimerization was experimentally carried out in toluene; in contrast, no solvent was employed for the cocyclization of alkynes/nitrile, but in the reaction mixture an excess of nitrile was present. Thus we have chosen to examine the effects of toluene and acetonitrile on both catalytic cycles. Since it has already been reported in a combined DFT and ^{103}Rh NMR study of numerous half-sandwich Rh(I) complexes that the solvation does not modify significantly the molecular structure,[43] solvent effects have been

(40) Yamamoto, Y.; Kinpara, K.; Ogawa, R.; Nishiyama, H.; Itoh, K. *Chem.−Eur. J.* **2006**, *12*, 5618.

(41) Caddy, P.; Green, M.; O'Brien, E.; Smart, L. E.; Woodward, P. *J. Chem. Soc., Dalton Trans.* **1980**, 962.

(42) A pure η^5 coordination, with five equivalent metal−C bonds, is not observed even in Cp derivatives: slippage of the ML_2 unit occurs, accompanied by folding of the ring: Albright, T. A.; Burdett, J. K.; Whangbo, M.-H. *Orbital Interactions in Chemistry*; Wiley: New York, 1985. In Ind complexes, the η^5 bonding mode is a distorted $\eta^3+\eta^2$ bonding mode. In fact, the nodal properties of the Ind π system introduce an asymmetry that is not present in the Cp π orbitals: Calhorda, M. J.; Veiros, L. F. *Coord. Chem. Rev.* **1999**, *185−186*, 37. In addition slippage toward a more allylic coordination in Ind complexes favors the aromatic character of the benzene ring. As a consequence, the two bonds of the metal to the hinge carbons are longer and weaker and both the slippage parameter and the folding angle of the five-membered ring are more pronounced in Ind complexes than in the analogous Cp complexes. These structural features are commonly invoked to explain the higher reactivity of Ind complexes than Cp complexes ("indenyl effect").

(43) Orian, L.; Bisello, A.; Santi, S.; Ceccon, A.; Saielli, G. *Chem.−Eur. J.* **2004**, *10*, 4029.

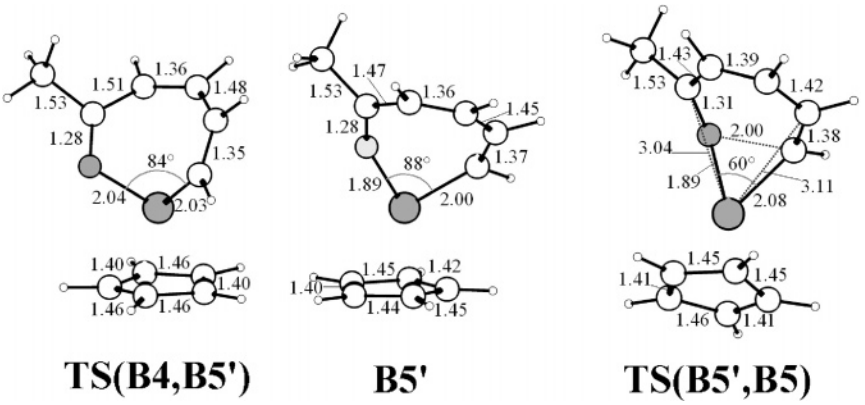

Figure 7. Structures of **TS(B4,B5′)**, **B5′**, and **TS(B5′,B5)** with selected interatomic distances (Å) and angles (deg).

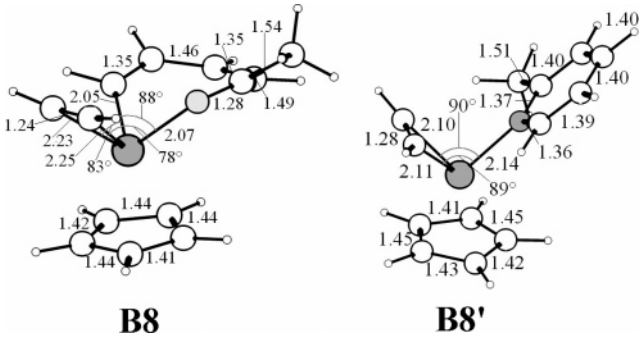

Figure 8. Structures of **B8** and **B8′** with selected interatomic distances (Å) and angles (deg).

accounted for by calculating the single-point energies of all the intermediates and transition states with the inclusion of the solvation correction, without carrying out the full geometry optimizations. The results are represented in Figure 11.

A larger solvent effect is observed in cycle B than in cycles A and C. In addition, acetonitrile has the largest stabilizing effect in all the cycles. The shift of the single-point energies calculated in solvent with respect to those calculated in vacuum is almost constant in cycle B. In contrast, in cycle A and, to a slightly minor extent, in cycle C, the solvent correction becomes less and less important and almost negligible for **A4** and **A5** (**C4** and **C5**).

In Figure 11 the energy barriers are indicated below each transition state data point. In cycle A the activation energy for the formation of the rhodacycle **A2** decreases from 12.7 kcal/mol in vacuum to 12.2 and 11.9 kcal/mol in toluene and acetonitrile, respectively; on the contrary the activation energy for the conversion **A3**−**A4** is almost unchanged (∼5 kcal/mol). In cycle B, in the presence of acetonitrile all the energy barriers are smaller than the corresponding values calculated in vacuum, while in toluene they are initially smaller, but the activation energies for the conversions **B4**−**B5** and **B5**−**B6** are higher than the corresponding values calculated in a vacuum. In cycle C the barrier of the rate-determining step decreases when going from the vacuum to toluene and acetonitrile. In contrast to what was observed for the conversion **A4**−**A5**, the energy barrier for the conversion **C4**−**C5** increases when going from the vacuum and toluene to acetonitrile.

The presence of the solvent slightly affects also the total amount of energy released in the process. For both the acetylene

Scheme 7. Energy Profile of the Cyclization of Three Acetylenes by the IndRh Fragment (energies in kcal/mol relative to the bisacetylene complex C1)

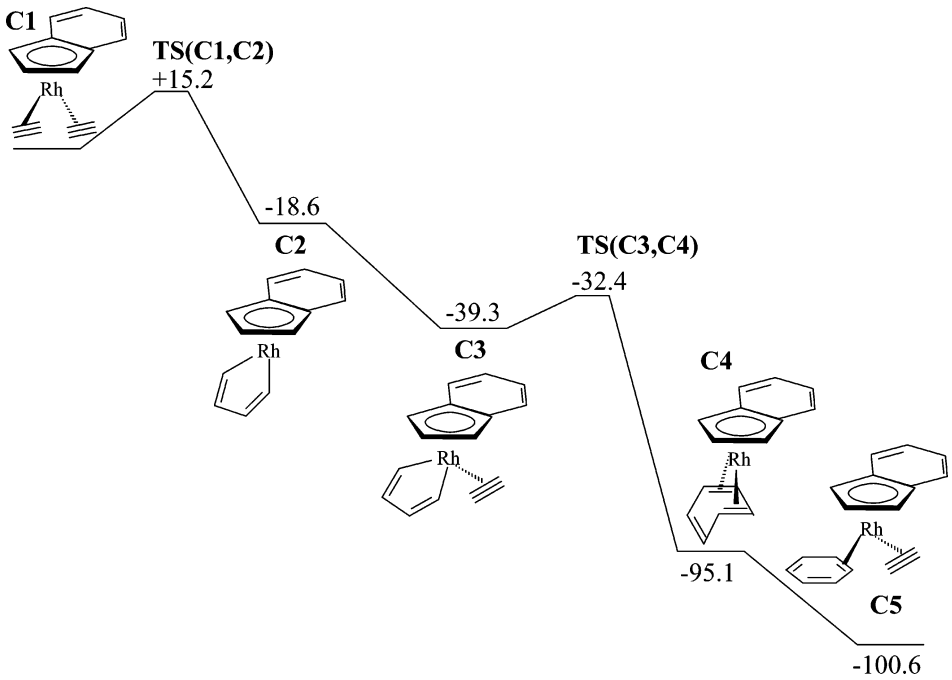

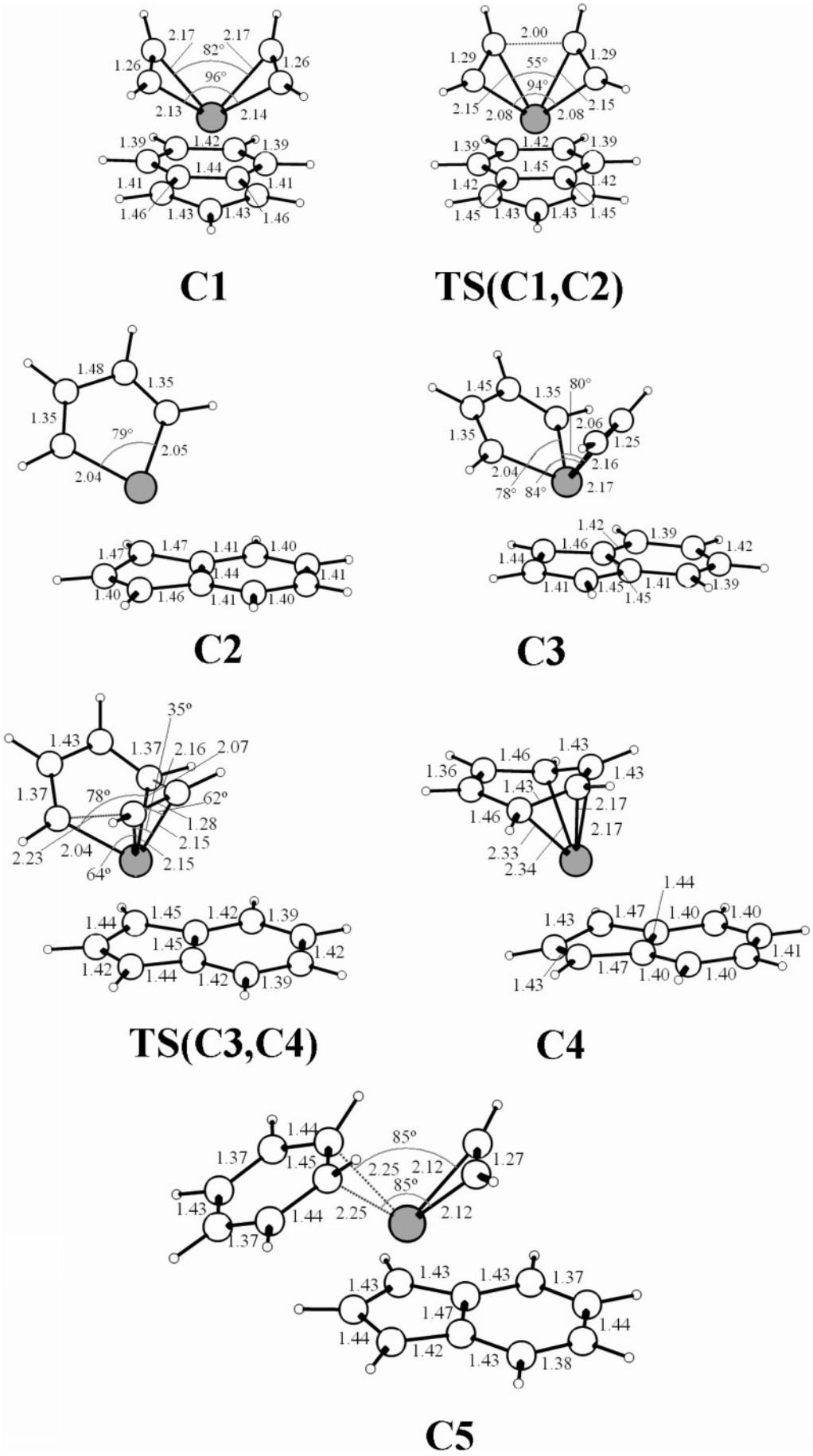

Figure 9. Structures of rhodium species shown in Scheme 7 with selected interatomic distances (Å) and angles (deg).

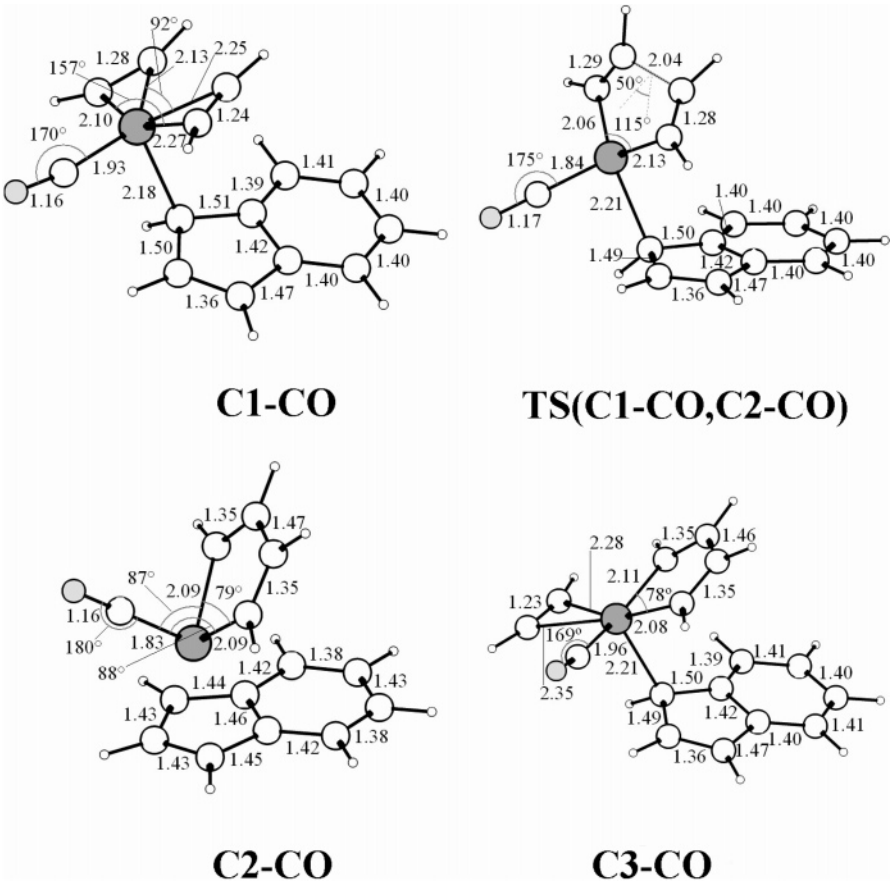

Figure 10. Structures of **C1-CO**, **TS(C1-CO,C2-CO)**, **C2-CO**, and **C3-CO** with selected interatomic distances (Å) and angles (deg).

trimerization to benzene and the cocyclization of acetylene and acetonitrile to 2-methylpyridine the value in toluene is slightly higher than the value estimated for the same process in acetonitrile, i.e., 118.6 (cycle A) versus 117.0 kcal/mol, 110.2 (cycle C) versus 108.7 kcal/mol, and 76.7 (cycle B) versus 74.2 kcal/mol. These values nicely compare with the corresponding energies calculated in vacuum, 125.8, 100.6, and 86.3 kcal/mol, respectively.

The analysis confirms that solvent effects have only a moderate influence on the studied mechanisms.

4. Conclusions

The mechanisms of the CpRh-catalyzed [2+2+2] cycloadditions of acetylene to benzene and of acetylene and acetonitrile to 2-methylpyridine have been theoretically explored using DFT calculations.

Both processes involve the formation of a coordinatively unsaturated 16-electron metallacycle, which has been identified as the rate-determining step. The barrierless coordination of a third acetylene molecule, and its subsequent addition to the π electron system of the rhodacycle, leads to an intermediate, which is characterized by a six-membered arene ring coordinated to the metal in η^4 fashion. The release of benzene occurs by stepwise addition of two acetylene molecules, which regenerates the catalyst. In the presence of acetonitrile, a nitrile molecule competes with acetylene to coordinate to the rhodacycle, to generate an intermediate that subsequently evolves to a peculiar bicyclic species. A few more stages are finally outlined for the formation and the eventual release of 2-methylpyridine.

Through a detailed description of the PESes we have rationalized the following:

(i) The competition between acetylene self-trimerization and acetylene/acetonitrile cocyclization: The formation of benzene is thermodynamically favored, in agreement with the experimental findings that an excess of nitrile is required to obtain good yields of pyridine. The coordination of acetonitrile to the five-membered rhodacycle can occur through σ-bonding, via the nitrogen lone-pair ("end-on"), and through π-bonding, with the nitrogen−carbon triple bond ("side-on"), and both intermediates have been connected to the subsequent bicyclic species. The route through the end-on coordination is thermodynamically favored, but the side-on intermediate is a more reactive complex.

(ii) The interplay between the size and the valence electron configuration of the metal core by comparing our results to those reported for CpCo- and CpRuCl-catalyzed acetylene cyclotrimerization: The mechanism of acetylene self-trimerization catalyzed by the CpRh fragment is essentially analogous to that described with CpCo as catalyst, but is slightly energetically disfavored. The existence of a bicyclic intermediate in the cocyclization process allows to establish an analogy also with the mechanisms catalyzed by CpRuCl, for which a similar intermediate was postulated. The seven-membered-ring species, which were located both on the PES of our CpRh-catalyzed acetylene self-trimerization and on the PES of our CpRh-catalyzed acetylene/acetonitrile cocyclization, are energetically disfavored intermediates and were thus excluded from the mechanisms; in contrast seven-membered-ring intermediates play a crucial role in CpRuCl-catalyzed trimerizations. These observations seem to indicate that the electronic structure of the metal core is more important than its size (covalent atomic radius) in controlling the mechanistic stages of the CpM-catalyzed processes.

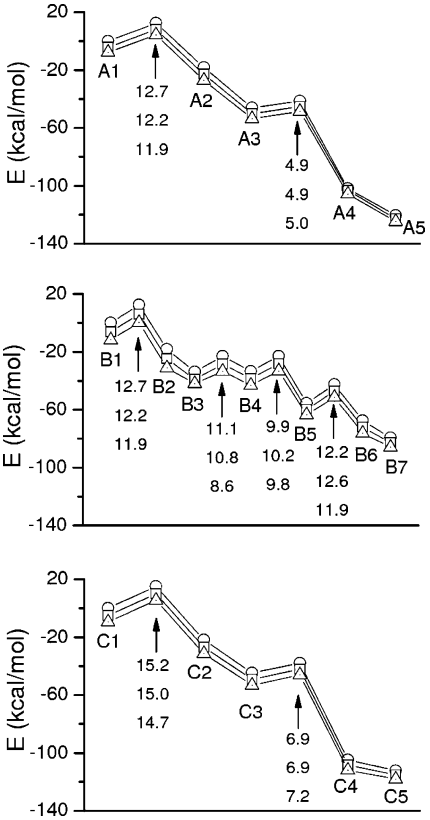

Figure 11. Solvent effects on the energies of the catalytic cycles A, B, and C: vacuum (open circles), toluene (open squares), and acetonitrile (open triangles). For a meaningful comparison the values of the energies in vacuum are not corrected for zero-point vibrational energy. The activation energies in kcal/mol are reported below each transition state data point (indicated with an arrow) in the order vacuum (top), toluene (middle), and acetonitrile (bottom).

(iii) The solvent effects: Solvent effects do not change significantly the qualitative aspects of the PESes and the mechanisms, likely due to the absence of charged or polarized intermediates.

The steric and electronic effects of the π ligand coordinated to the metal have also been included in our exploration by addressing the mechanism of the IndRh-catalyzed acetylene self-trimerization to benzene. We have found that the catalytic path of acetylene homotrimerization with the IndRh fragment is similar to that described with the CpRh fragment. Surprisingly, no evidence of the "indenyl effect" was found and the IndRh-catalyzed cycle with the chosen reactants is less efficient than the CpRh-catalyzed process, likely due to the less efficient donor character and larger steric demand of the indenyl ligand.

Acknowledgment. This work has been performed under the Project HPC-EUROPA (RII3-CT-2003-506079), with the support of the European Union−Research Infrastructure Action under the FP6 "Structuring the European Research Area" Programme. We also thank the Netherlands Organization for Scientific Research (NWO-CW and NWO-NCF) for financial support. The calculations were carried out on Teras and Aster parallel machines of SARA (Amsterdam) and on the TC cluster of the Vrije Universiteit. L.O. acknowledges Prof. Alberto Ceccon (University of Padova, Italy), who first introduced her into the field of rhodium chemistry and for his precious comments on her HPC proposal. The authors are grateful to Prof. Giovanni Ingrosso (University of Pisa, Italy) for the enlightening discussion of the experimental aspects and for carefully reading and commenting on the manuscript.

Supporting Information Available: Cartesian coordinates, total energies and selected structural parameters for all the calculated intermediates and transition states; calculated single imaginary frequencies of the transition states; rhodium atomic charges; selected structural parameters of the crystallographic structures of several CpRh complexes taken from CSD; complete ref 15b. This material is available free of charge via the Internet at http://pubs.acs.org.

OM7004222